A Comparison Between Robust Control Design LMIs for Grid-Connected Converters

Gustavo G. Koch
Federal University of Rio Grande do Sul – UFRGS
Porto Alegre, RS, Brazil

Caio R. D. Osório and Vinícius F. Montagner
Federal University of Santa Maria – UFSM
Santa Maria, RS, Brazil

***Abstract*—This paper is focused on a comparison between two linear matrix inequality conditions for design of robust state feedback controllers applied for current regulation of grid-connected converters with LCL filters, operating under uncertain grid impedance at the point of common coupling. The first condition is the well known quadratic stability and the second one is the polyquadratic stability, which uses extra matrix variables. It is shown that the condition with slack variables can provide superior performance in terms of ensuring stable and suitable operation for a larger set of uncertainties.**

***Keywords* – Grid-connected converters, Linear matrix inequalities, Robust control, Robust stability, Uncertain systems.**

I. Introduction

Grid-connected converters (GCCs) are fundamental in distributed generation systems, allowing, for instance, to control the power flow between renewable energy sources and the grid [1]–[3]. Several control techniques have been employed to ensure grid injected currents respecting limits of harmonic distortion. Considering the linear current control methods with pulse-width modulation (PWM), one has the important strategies based on integral action (e.g. proportional integral controllers in dq coordinates [4], [5]) and on resonant action (e.g. proportional resonant controllers in $\alpha\beta$ coordinates [6], [7]).

One important stage in a GCC is a filter between the inverter and the grid, in order to attenuate the high frequency harmonics from the PWM voltages generated by the inverter. In this context, LCL filters have been widely used due to the attenuation profile with -60 dB per decade [8], [9]. However, such filters have a challenge of presenting a resonance peak that must be attenuated, in order to avoid loss of performance or even instability. This problem is more challenging due to the fact that, when the LCL filter is connected to a grid with uncertain impedance in the point of common coupling (PCC), the resonance frequency may vary inside a large interval. Thus, controllers designed to attenuate the LCL resonance at a specific frequency may not work properly. This fact demands more efficient control designs, capable to stabilize marginally stable plants subject to uncertain parameters. In this scenario, state feedback controllers designed by means of linear matrix inequalities (LMIs) have been successfully applied to GCCs with LCL filters subject to uncertain grid impedances [10]–[16].

Although the LMI framework is recognized as highly efficient in computational point of view to deal with robust control of GCCs, there is a lack of works in the literature comparing different LMIs in the solution of robust control design for GCCs under uncertain grid impedances. The control theory literature shows that less conservative LMIs such as those based on extra matrix variables can provide better performance [17], [18]. The theoretical comparisons between LMIs are carried out, in general, in a scenario without limitations in the control signal. In the case of practical application of control for GCCs, the control signal is limited and this fact can be taken into account in a comparative study of performance of different LMI based controllers applied in practice.

This paper provides a comparison between two LMI robust control design conditions applied to GCCs with LCL filters, with grid predominantly inductive, and whose inductance is uncertain, lying on a given interval. First, a polytopic model of the GCC is given, taking into account the uncertain parameters and the delay from a digital control implementation. Second, two LMIs are presented, in order to provide the robust state feedback control gains. These LMIs are based on the quadratic stability and on the polyquadratic stability. Third, the performance with these robust control gains is compared in a scenario with limitations in the control signal and it is shown that one can have better performance with the more relaxed LMI design.

II. Modeling

Consider the three-phase inverter connected to the PCC by means of an LCL filter, as illustrated in Figure 1. The controller is developed in $\alpha\beta$ coordinates, as described in the sequence. It is also assumed that the voltages at the PCC are measured and the synchronism with the grid voltage is ensured by a suitable algorithm.

The grid is assumed as predominantly inductive and possibly time-varying [19], [20]. The grid inductance L_{g2} belongs to a bounded interval for which only the maximum and minimum values are given. Therefore, for a balanced three-phase system, one can write, for any of the three phases, that

$$L_g = L_{g1} + L_{g2} \tag{1}$$

The plant depicted in Figure 1 can be represented by a state space model in stationary reference frame. Assuming a balanced system, and that there is no path for the current

https://doi.org/10.53316/sepoc2021.054

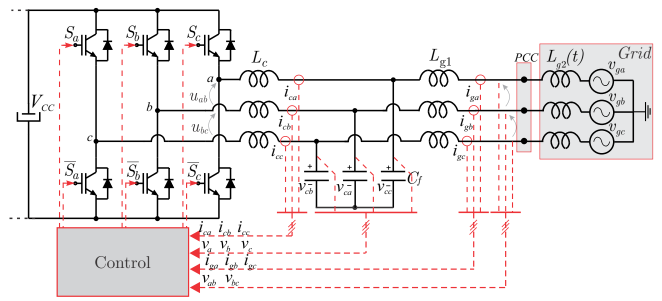

Figure 1. Three-phase inverter connected to the grid by means of an LCL filter.

of axis $'0'$, the system can be described by means of two uncoupled single-phase systems, given by [21]

$$\begin{array}{l}\dot{\boldsymbol{x}}_\alpha=\boldsymbol{A}(L_g)\boldsymbol{x}_\alpha+\boldsymbol{B}_u u_\alpha+\boldsymbol{B}_d(L_g)v_{g\alpha}\\ \dot{\boldsymbol{x}}_\beta=\boldsymbol{A}(L_g)\boldsymbol{x}_\beta+\boldsymbol{B}_u u_\beta+\boldsymbol{B}_d(L_g)v_{g\beta}\end{array}\tag{2}$$

where

$$\begin{array}{l}\boldsymbol{A}(L_g)=\begin{bmatrix}0 & \frac{-1}{L_c} & 0\\ \frac{1}{C_f} & 0 & \frac{-1}{C_f}\\ 0 & \frac{1}{L_g} & 0\end{bmatrix},\ \boldsymbol{B}_u=\begin{bmatrix}\frac{1}{L_c}\\ 0\\ 0\end{bmatrix},\\ \boldsymbol{B}_d(L_g)=\begin{bmatrix}0\\ 0\\ \frac{-1}{L_g}\end{bmatrix},\ \boldsymbol{x}_\alpha=\begin{bmatrix}i_{c\alpha}\\ v_{c\alpha}\\ i_{g\alpha}\end{bmatrix},\ \boldsymbol{x}_\beta=\begin{bmatrix}i_{c\beta}\\ v_{c\beta}\\ i_{g\beta}\end{bmatrix}\end{array}\tag{3}$$

In this representation, $i_{c\alpha}$ is the current through the converter-side inductor, $v_{c\alpha}$ is the voltage across the filter capacitor, and $i_{g\alpha}$ is the current injected into the grid. The same reasoning is valid for axis β.

For the application of a digital control law, consider the discretization of the plant with a sufficiently small sampling period T_s, and also the inclusion of an additional state, ϕ, representing the one sample digital delay. The discretized model is given by [1]

$$\begin{array}{l}\boldsymbol{x}(k+1)=\boldsymbol{A}_d(\boldsymbol{\theta})\boldsymbol{x}(k)+\boldsymbol{B}_{ud}(\boldsymbol{\theta})\phi(k)+\boldsymbol{B}_{dd}(\boldsymbol{\theta})v_g(k)\\ \phi(k+1)=u(k)\\ y(k)=\boldsymbol{C}_y\boldsymbol{x}(k)=[0\ 0\ 1]\boldsymbol{x}(k)=i_g(k)\end{array}\tag{4}$$

To obtain the matrices in model (4), the continuous-time matrices in (3) were discretized for each extreme value of L_g, and then convexically combined, leading to [22]

$$\begin{array}{l}(\boldsymbol{A}_d,\boldsymbol{B_{ud}},\boldsymbol{B_{dd}})(\boldsymbol{\theta})=\sum\limits_{j=1}^{2}\theta_j(\boldsymbol{A}_{dj},\boldsymbol{B}_{udj},\boldsymbol{B}_{ddj}),\ [\theta_1,\theta_2]\in\Theta,\\ \Theta\triangleq\{\boldsymbol{\theta}\in\mathbb{R}^2:\theta_1+\theta_2=1,\theta_j\geq 0,\ j=1,2\}\end{array}\tag{5}$$

in which

$$\boldsymbol{A}_{dj}=e^{\boldsymbol{A}_jT_s},\boldsymbol{B}_{udj}=\int\limits_0^{T_s}e^{\boldsymbol{A}_j\tau}\boldsymbol{B}_u d\tau,\boldsymbol{B}_{ddj}=\int\limits_0^{T_s}e^{\boldsymbol{A}_j\tau}\boldsymbol{B}_{dj}d\tau\tag{6}$$

[1]From this point on, for simplicity, the subscripts α and β are suppressed.

with

$$\begin{array}{ll}\boldsymbol{A}_1=\boldsymbol{A}(L_{gmin}), & \boldsymbol{A}_2=\boldsymbol{A}(L_{gmax}),\\ \boldsymbol{B}_{d1}=\boldsymbol{B}_d(L_{gmin}), & \boldsymbol{B}_{d2}=\boldsymbol{B}_d(L_{gmax}).\end{array}\tag{7}$$

To ensure tracking of sinusoidal references and rejection of harmonic disturbances, n resonant controllers are included in the model, leading to the representation [12]

$$\boldsymbol{\xi}(k+1)=\boldsymbol{R}\boldsymbol{\xi}(k)+\boldsymbol{T}(i_{ref}(k)-y(k))\tag{8}$$

where

$$\boldsymbol{\xi}=\begin{bmatrix}\boldsymbol{\xi}_1\\ \vdots\\ \boldsymbol{\xi}_n\end{bmatrix},\ \boldsymbol{R}=\begin{bmatrix}\boldsymbol{R}_1 & & \\ & \ddots & \\ & & \boldsymbol{R}_n\end{bmatrix},\ \boldsymbol{T}=\begin{bmatrix}\boldsymbol{T}_1\\ \vdots\\ \boldsymbol{T}_n\end{bmatrix}\tag{9}$$

and i_{ref} is the reference for the grid currents. $\boldsymbol{\xi}$, $\boldsymbol{R}$ and $\boldsymbol{T}$ are, respectively, the state vector and the matrices of the multiple resonant controllers. Each vector $\boldsymbol{\xi}_i$, $i=1...n$, has two states and represents one resonant controller.

Notice that (4)-(8) can be rewritten as

$$\begin{array}{l}\begin{bmatrix}\boldsymbol{x}(k+1)\\ \phi(k+1)\\ \boldsymbol{\xi}(k+1)\end{bmatrix}=\begin{bmatrix}\boldsymbol{A}_d(\boldsymbol{\theta}) & \boldsymbol{B}_{ud}(\boldsymbol{\theta}) & \mathbf{0}_{3\times 2n}\\ \mathbf{0}_{1\times 3} & 0 & \mathbf{0}_{1\times 2n}\\ -\boldsymbol{T}_{2n\times 1}\boldsymbol{C}_y & \mathbf{0}_{2n\times 1} & \boldsymbol{R}_{2n\times 2n}\end{bmatrix}\begin{bmatrix}\boldsymbol{x}(k)\\ \phi(k)\\ \boldsymbol{\xi}(k)\end{bmatrix}+\\ +\begin{bmatrix}\mathbf{0}_{3\times 1}\\ 1\\ \mathbf{0}_{2n\times 1}\end{bmatrix}u(k)+\begin{bmatrix}\boldsymbol{B}_{dd}(\boldsymbol{\theta})\\ 0\\ \mathbf{0}_{2n\times 1}\end{bmatrix}v_g(k)+\begin{bmatrix}\mathbf{0}_{3\times 1}\\ 0\\ \boldsymbol{T}_{2n\times 1}\end{bmatrix}i_{ref}(k)\end{array}\tag{10}$$

or, in a more compact form, as

$$\begin{array}{l}\boldsymbol{\rho}(k+1)=\boldsymbol{G}(\boldsymbol{\theta})\boldsymbol{\rho}(k)+\boldsymbol{H}_u u(k)+\boldsymbol{H}_d(\boldsymbol{\theta})v_g(k)\\ \qquad+\boldsymbol{H}_{ref}i_{ref}(k)\\ y(k)=\boldsymbol{C}\boldsymbol{\rho}(k),\ \boldsymbol{C}=\begin{bmatrix}\boldsymbol{C}_y & \mathbf{0}_{1\times(2n+1)}\end{bmatrix}\end{array}\tag{11}$$

where

$$\boldsymbol{G}(\boldsymbol{\theta})=\sum_{j=1}^{2}\theta_j\boldsymbol{G}_j,\ \ \boldsymbol{H}_d(\boldsymbol{\theta})=\sum_{j=1}^{2}\theta_j\boldsymbol{H}_{dj}\tag{12}$$

with $[\theta_1,\theta_2]\in\Theta$, $\forall k\geq 0$.

This model is suitable to design robust state feedback controllers by means of LMIs (see, for instance, [12]–[14]).

III. Control design based on LMIs

Consider that the state feedback control law

$$u(k)=\boldsymbol{K}\boldsymbol{\rho}(k)=\begin{bmatrix}\boldsymbol{K}_x & K_\phi & \boldsymbol{K}_\xi\end{bmatrix}\begin{bmatrix}\boldsymbol{x}(k)\\ \phi(k)\\ \boldsymbol{\xi}(k)\end{bmatrix}\tag{13}$$

is applied to the system (11).

The state feedback controller gains can be computed using the robust stabilizability LMIs based on quadratic stability and on polyquadratic stability given below.

1) Quadratic stability [23]: If there exist $\mathcal{W}$ and $\mathcal{Z}$ for all $i=1,2$, such that

$$\mathcal{W}=\mathcal{W}'>\mathbf{0}\tag{14}$$

$$\begin{bmatrix}\mathcal{W} & \mathcal{W}\boldsymbol{G}_i{}'+\mathcal{Z}'\boldsymbol{H}_{ui}{}'\\ \boldsymbol{G}_i\mathcal{W}+\boldsymbol{H}_{ui}\mathcal{Z} & \mathcal{W}\end{bmatrix}>\mathbf{0}\tag{15}$$

then the state feedback control gain vector

$$\boldsymbol{K} = \boldsymbol{\mathcal{Z}}\boldsymbol{\mathcal{W}}^{-1} \tag{16}$$

ensures the asymptotic stability of the closed-loop system.

2) Polyquadratic stability [24]: If there exist symmetric positive definite matrices $\boldsymbol{\mathcal{S}}_j$, $j = 1, 2$, and matrices $\boldsymbol{\mathcal{G}}$ and $\boldsymbol{\mathcal{R}}$ such that the following LMIs[2]

$$\begin{bmatrix} \boldsymbol{\mathcal{G}} + \boldsymbol{\mathcal{G}}' - \boldsymbol{\mathcal{S}}_j & \boldsymbol{\mathcal{G}}'\boldsymbol{G}_j' + \boldsymbol{\mathcal{R}}'\boldsymbol{H}_{uj}' \\ \boldsymbol{G}_j\boldsymbol{\mathcal{G}} + \boldsymbol{H}_{uj}\boldsymbol{\mathcal{R}} & \boldsymbol{\mathcal{S}}_i \end{bmatrix} > 0 \quad \begin{matrix} i = 1, 2 \\ j = 1, 2 \end{matrix} \tag{17}$$

hold, then the state feedback control gain vector given by

$$\boldsymbol{K} = \boldsymbol{\mathcal{R}}\boldsymbol{\mathcal{G}}^{-1} \tag{18}$$

ensures the asymptotic stability of the closed-loop system. [12].

To allow a comparative study of these control design LMIs, consider for a case study the GCC borrowed from the literature [13], [14], [16], whose parameters are shown in Table I. Notice that the grid inductance is given here by an uncertain interval of L_{g2} from 0 mH to 3 mH. Notice also that there are four resonant controllers, chosen in terms of frequency and damping factor as in the previous mentioned references.

Table I
SYSTEM PARAMETERS.

Converter inductance L_c	1 mH
Filter capacitor C_f	62 μH
Grid-side inductance L_{g1}	0.3 mH
Grid inductance L_{g2}	[0 mH ; 3 mH]
Sampling frequency T_s	1/20040 s
Switching frequency	1/10020 s
Grid phase voltage	127 Vrms; 60 Hz
DC-link	400 V
Resonant frequencies	60, 180, 300 and 420 Hz
Resonant damping factor	0.0001

Applying the LMIs in this section for the set of parameters in Table I, one has that both LMIs are feasible. The quadratic stability leads to the gains K'_{QS}, while the polyquadratic stability, based on extra matrix variables, leads to the gains K'_{PQS} in Table II [3].

Although both conditions provide control gains, the viability of the closed-loop control system with these gains must be evaluated under limitations of the control signal, which were not taken into account in the control design stage. In this direction, simulations for control validation are given in the next section.

IV. SIMULATIONS AND CONTROL VALIDATION

In order to validate the control gains in conditions closer of practical application, tests of sinusoidal reference tracking for

[2]The value of n represents the number of resonant controllers, that is, if four resonant controllers are used, and $n = 4$ then $\boldsymbol{K}$ belongs to $\mathbb{R}^{1\times 12}$.

[3]Gains obtained by means the solver *LMI control toolbox* (MATLAB®)

Table II
CONTROL GAINS.

$\boldsymbol{K}'_{QS}$	$\boldsymbol{K}'_{PQS}$
-22.74189048	-17.20640173
-8.27935946	-5.11265162
-9.83442208	-6.16577797
-1.00034347	-0.73197371
63.56200269	51.33879276
-63.45499580	-51.17310062
21.30606037	17.31028709
-22.40198848	-18.02405838
14.88119349	11.66425868
-18.45408436	-14.01190485
11.99894623	9.07983549
-19.21054987	-13.84923202

the closed-loop system with limitations in the control signal, which is implemented as PWM waveforms of amplitude 400 V and frequency of 20040 Hz, are taken into account. The reference signal for grid currents in α and β axes begins with zero value, then is changed to 10 A of peak value. Two changes in the phase of the reference are imposed and finally a change in the amplitude of the reference, to the peak value of 20 A, is implemented.

Considering the gains K'_{QS} in Table II, designed with the quadratic stability, Figure 2 shows the grid current reference in α and the respective controlled grid-current and Figure 3 shows the respective control signal. In this simulation, the output of the control system progressively increases in amplitude, indicating the instability in practice with for the grid operation condition of $L_{g2} = 0$ mH, that is, for strong grid condition. Thus, a limitation with the design with the quadratic stability can be observed.

On the other hand, the polyquadratic stability, with control

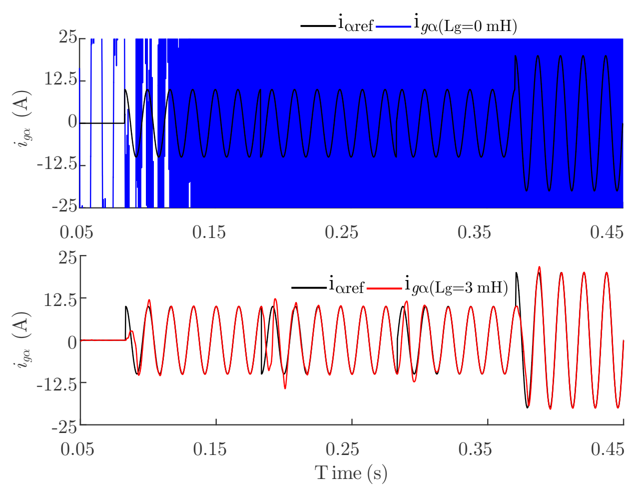

Figure 2. Closed-loop responses with the control gains from the quadratic stability. Top: operation at $L_{g2} = 0$ mH (instability). Bottom: operation at $L_{g2} = 3$ mH.

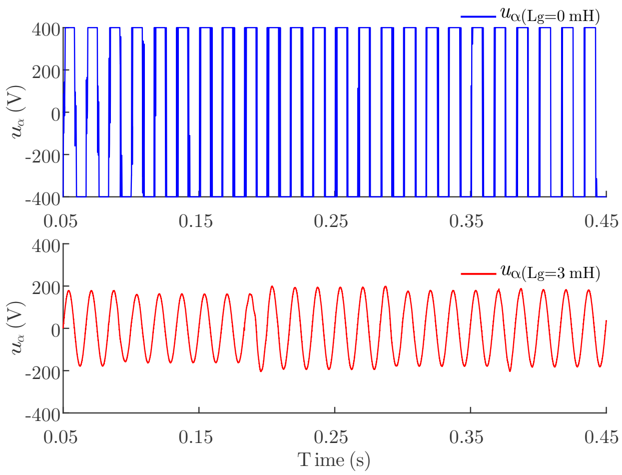

Figure 3. Control signals from Figure 2.

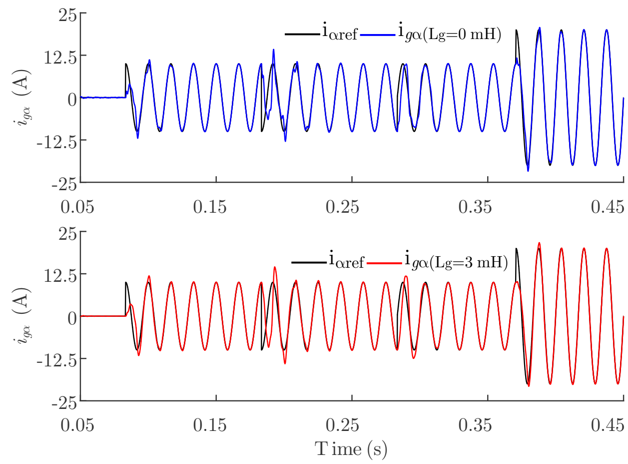

Figure 4. Closed-loop responses with the control gains from the polyquadratic stability. Top: operation at $L_{g2} = 0$ mH. Bottom: operation at $L_{g2} = 3$ mH.

gains K'_{PQS} in Table II, ensures stable operation for the entire range of grid inductance values, as can be verified in figures 4 and 5, for the extreme values of $L_{g2} = 0$ mH and $L_{g2} = 3$ mH. Notice the suitable transient responses under the amplitude and phase changes of the reference signal, and also the good steady state performance, with the controllers designed with the more relaxed LMI design conditions.

It is worth to mention that the polyquadratic stability leads to better results than the quadratic stability in this case due to the fact that the control gains of the quadratic stability tend to increase to keep the poles inside the unit circle for the large interval of L_{g2} under consideration here, as can be seen comparing the gains $\boldsymbol{K}'_{QS}$ and $\boldsymbol{K}'_{PQS}$ in Table II. Both gains would be sufficient to ensure stability under linear operation of the converter. However, in practice, the control action is limited in amplitude and in frequency, and then the larger gains, from quadratic stability, are not viable in this case study. On the other hand, due to extra variables in the design problem, the polyquadratic stability produces control gains that avoid problems with limitation in the control signal, leading to viable results.

In order to corroborate the good performance of the closed-loop system with the gains designed by the polyquadratic stability, Figure 6 shows the Bode diagrams from the reference to the output i_g, where one can verify the 0 dB gain and phase equivalent to 0 degrees, thus confirming the good reference tracking capacity of the closed-loop system.

A sweep in the closed-loop poles of the system with gains designed by the polyquadratic stability are given in Figure 7, confirming the theoretical stability for the entire grid inductance interval value, based on the models shown in Section II.

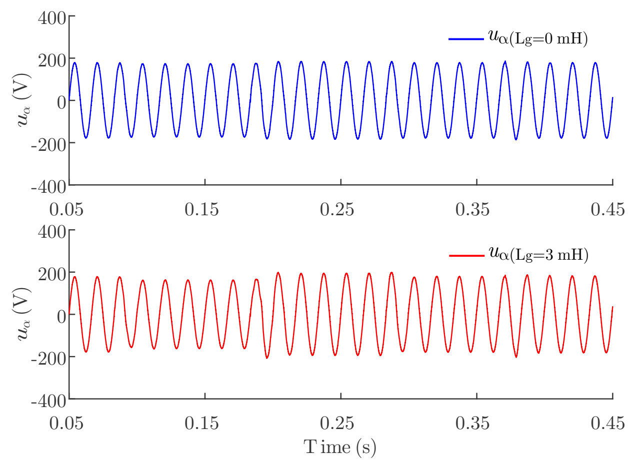

Figure 5. Control signals from Figure 4.

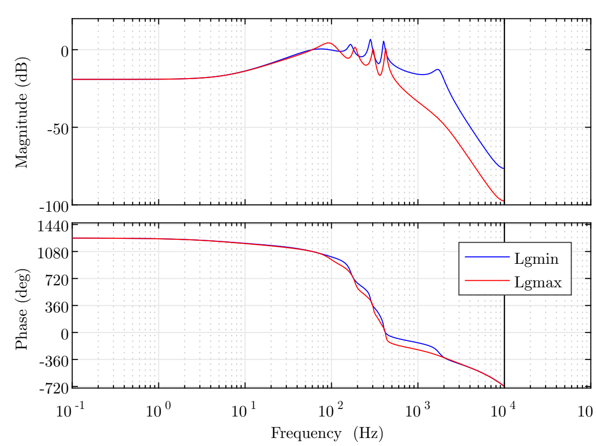

Figure 6. Bode diagrams from the reference signal to the output signal, for the closed-loop system with the polyquadratic stability gains, for both extreme values of the grid inductance.

V. Conclusion

This paper explored two LMI conditions for robust control design applied to GCCs operating under uncertain grid impedance at the PCC. The first condition, known as quadratic stability, has two matrix variables, that are used to recover the state feedback control gains vector. The second condition, known as polyquadratic stability, has four matrix variables,

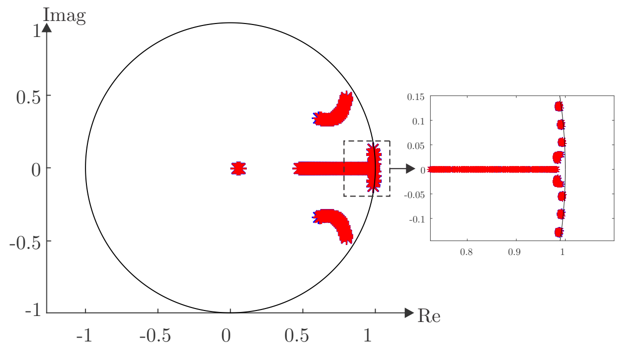

Figure 7. Closed-loop poles of the system with the polyquadratic stability gains, for a large set of values inside the grid inductance interval from 0 mH to 3 mH.

thus including additional variables which improve the control design solution. A case study for a GCC with LCL filter connected to a predominantly inductive grid was shown, for both LMI design conditions. The converter was modeled including grid parameter uncertainty in a real interval and one step control implementation delay. The resulting control gains illustrate a case where the quadratic stability gains cannot ensure stability for a large interval of grid inductances, due to the higher conservativeness of these LMIs for system with larger intervals of uncertainty. On the other hand, thanks to the extra matrix variables and the lower conservativeness when compared to the quadratic stability, the polyquadratic stability provides, for this case study, a set of gains capable of ensuring stability and good performance, thus indicating that relaxed LMIs can be explored to provide results with a good tradeoff between robustness and performance for GCC applications.

VI. Acknowledgments

This study was financed in part by the Coordenação de Aperfeiçoamento de Pessoal de Nível Superior - Brasil (CAPES/PROEX) - Finance Code 001. The authors also thank to INCT-GD, CNPq (465640/2014-1 and 309536/2018-9), CAPES (23038.000776/2017-54) and FAPERGS (17/2551-0000517-1).

References

[1] R. Teodorescu, M. Liserre, and P. Rodríguez, *Grid Converters for Photovoltaic and Wind Power Systems*, ser. Wiley - IEEE. John Wiley & Sons, 2011.

[2] R. W. Erickson, *Fundamentals of Power Electronics*. New York, NY: Chapman & Hall, 1997.

[3] F. Blaabjerg, Z. Chen, and S. Kjaer, "Power Electronics as Efficient Interface in Dispersed Power Generation Systems," *IEEE Transactions on Power Electronics*, vol. 19, no. 5, pp. 1184–1194, Sept 2004.

[4] J. Dannehl, F. Fuchs, and P. Thøgersen, "PI State Space Current Control of Grid-Connected PWM Converters With LCL Filters," *IEEE Transactions on Power Electronics*, vol. 25, no. 9, pp. 2320 –2330, sept. 2010.

[5] J. Dannehl, M. Liserre, and F. Fuchs, "Filter-Based Active Damping of Voltage Source Converters With LCL Filter," *IEEE Transactions on Industrial Electronics*, vol. 58, no. 8, pp. 3623 –3633, August 2011.

[6] R. Teodorescu, F. Blaabjerg, M. Liserre, and P. Loh, "Proportional-Resonant Controllers and Filters for Grid-Connected Voltage-Source Converters," *Electric Power Applications, IEE Proceedings*, vol. 153, no. 5, pp. 750–762, September 2006.

[7] M. Liserre, R. Teodorescu, and F. Blaabjerg, "Multiple Harmonics Control for Three-Phase Grid Converter Systems with the use of PI-RES Current Controller in a Rotating Frame," *Power Electronics, IEEE Transactions on*, vol. 21, no. 3, pp. 836–841, May 2006.

[8] R. Peña-Alzola, M. Liserre, F. Blaabjerg, R. Sebastián, J. Dannehl, and F. W. Fuchs, "Analysis of the Passive Damping Losses in LCL-Filter-Based Grid Converters," *IEEE Transactions on Power Electronics*, vol. 28, no. 6, pp. 2642 –2646, june 2013.

[9] A. Timbus, M. Liserre, R. Teodorescu, P. Rodriguez, and F. Blaabjerg, "Evaluation of Current Controllers for Distributed Power Generation Systems," *Power Electronics, IEEE Transactions on*, vol. 24, no. 3, pp. 654–664, march 2009.

[10] I. J. Gabe, V. F. Montagner, and H. Pinheiro, "Design and Implementation of a Robust Current Controller for VSI Connected to the Grid Through an LCL Filter," *IEEE Transactions on Power Electronics*, vol. 24, no. 6, pp. 1444–1452, June 2009.

[11] L. A. Maccari, Jr., J. R. Massing, L. Schuch, C. Rech, H. Pinheiro, R. C. L. F. Oliveira, and V. F. Montagner, "LMI-Based Control for Grid-Connected Converters With LCL Filters Under Uncertain Parameters," *IEEE Transactions on Power Electronics*, vol. 29, no. 7, pp. 3776–3785, July 2014.

[12] L. A. Maccari, H. Pinheiro, R. C. Oliveira, and e Vinícius F. Montagner, "Robust Pole Location with Experimental Validation for Three-Phase Grid-Connected Converters," *Control Engineering Practice*, vol. 59, pp. 16 – 26, 2017.

[13] G. G. Koch, L. A. Macari, R. Oliveira, and V. F. Montagner, "Robust $\mathcal{H}_\infty$ State Feedback Controllers based on LMIs applied to Grid-Connected Converters," *IEEE Transactions on Industrial Electronics*, vol. 66, no. 8, pp. 6021–6031, 2019.

[14] C. R. Osório, G. G. Koch, R. C. Oliveira, and V. F. Montagner, "A Practical Design Procedure for Robust $\mathcal{H}_2$ Controllers Applied to Grid-Connected Inverters," *Control Engineering Practice*, vol. 92, p. 104157, 2019.

[15] C. R. D. Osório, G. G. Koch, H. Pinheiro, R. C. L. F. Oliveira, and V. F. Montagner, "Robust Current Control of Grid-Tied Inverters Affected by LCL Filter Soft-Saturation," *IEEE Transactions on Industrial Electronics*, vol. 67, no. 8, pp. 6550–6561, August 2019.

[16] G. G. Koch, C. R. D. Osório, H. Pinheiro, R. C. L. F. Oliveira, and V. F. Montagner, "Design Procedure Combining Linear Matrix Inequalities and Genetic Algorithm for Robust Control of Grid-Connected Converters," *IEEE Transactions on Industry Applications*, vol. 56, no. 2, pp. 1896–1906, 2020.

[17] R. C. Oliveira and P. L. Peres, "LMI Conditions for Robust Stability Analysis Based on Polynomially Parameter-Dependent Lyapunov Functions," *Systems & Control Letters*, vol. 55, no. 1, pp. 52 – 61, 2006.

[18] R. C. L. F. Oliveira, M. C. de Oliveira, and P. L. D. Peres, "Parameter-Dependent Lyapunov Functions for Robust Stability Analysis of Time-Varying Systems in Polytopic Domains," in *Proceedings of the 2007 American Control Conference*, New York, NY, July 2007.

[19] Q. Liu, T. Caldognetto, and S. Buso, "Stability Analysis and Auto-Tuning of Interlinking Converters Connected to Weak Grids," *IEEE Transactions on Power Electronics*, vol. 34, no. 10, pp. 9435–9446, 2019.

[20] C. S. Lim, S. S. Lee, I. U. Nutkani, X. Kong, and H. H. Goh, "Near-Optimal MPC Algorithm for Actively Damped Grid-Connected PWM-VSCs With LCL Filters," *IEEE Transactions on Industrial Electronics*, vol. 67, no. 6, pp. 4578–4589, 2020.

[21] W. Duesterhoeft, M. W. Schulz, and E. Clarke, "Determination of Instantaneous Currents and Voltages by Means of Alpha, Beta, and Zero Components," *American Institute of Electrical Engineers, Transactions of the*, vol. 70, no. 2, pp. 1248–1255, July 1951.

[22] S. Boyd, L. El Ghaoui, E. Feron, and V. Balakrishnan, *Linear Matrix Inequalities in System and Control Theory*. Philadelphia, PA: SIAM Studies in Applied Mathematics, 1994.

[23] J. Bernussou, P. L. D. Peres, and J. C. Geromel, "A Linear Programming Oriented Procedure for Quadratic Stabilization of Uncertain Systems," *Systems & Control Letters*, vol. 13, no. 1, pp. 65–72, July 1989.

[24] J. Daafouz and J. Bernussou, "Parameter Dependent Lyapunov Functions for Discrete Time Systems with Time Varying Parameter Uncertainties," *Systems & Control Letters*, vol. 43, no. 5, pp. 355–359, August 2001.